View metadata, citation and similar papers at core.ac.uk

brought to you by CORE

provided by Elsevier - Publisher Connector

International Journal of Solids and Structures 47 (2010) 1871–1875

Contents lists available at ScienceDirect

International Journal of Solids and Structures

journal homepage: www.elsevier.com/locate/ijsolstr

Study on the generalized thermoelastic vibration of the optically excited semiconducting microcantilevers

Yaqin Song [a,b,d,*], Dragan M. Todorovic [c,d], Bernard Cretin [d], Pascal Vairac [d]

[a] MOE Key Laboratory for Strength and Vibration, School of Aerospace, Xi'an Jiaotong University, 710049 Xi'an, People's Republic of China
[b] State Key Laboratory of Structural Analysis for Industrial Equipment, Dalian University of Technology, Dalian 116023, People's Republic of China
[c] Institute for multidisciplinary researches, University of Belgrade, K.Viseslava 1, 11030 Belgrade, Serbia
[d] FEMTO-ST, Université de Franche-Comté, CNRS, ENSMM, UTBM, 32 Avenue de l'Observatoire, 25044 Besançon Cedex, France

ARTICLE INFO

Article history:
Received 15 June 2009
Received in revised form 17 March 2010
Available online 27 March 2010

Keywords:
Photothermal
Thermoelasticitic wave
Plasma wave
Semiconducting microcantilever
Vibration

ABSTRACT

In this paper, the theory of coupled plasma, thermal and elastic wave was used to study the vibration of semiconducting microcantilevers during photothermal process. The generalized thermoelastic model was adopted, along with plasma wave model, to obtain the vibration response of semiconducting microcantilevers under periodical laser excitation. The influence of thermal relaxation time on the vibration was investigated. The conventional and generalized thermoelastic theories for the temperature and deflection of microcantilever were compared. The simulation results for the amplitude and phase versus the modulation frequency revealed that near resonance frequency the generalized hyperbolic thermoelastic model was more suitable to describe the vibration characterization of microcantilevers than the conventional thermoelstic model.

© 2010 Elsevier Ltd. All rights reserved.

1. Introduction

The development and utilization of microcantilevers have increased considerably within the past few years because of their low cost and high sensitivity as measurement and detection probes. Thus the study of the response of microcantilevers under different excitations (thermal, mechanical, photothermal, photoacoustic, piezoelectric etc.,) becomes a very important topic. Many researchers have endeavored to investigate the behavior and characteristics of microcantilevers experimentally or theoretically, or both. Here we only mention some works in recent years. In order to improve the force sensitivity and time response of dynamic force microscopy, Fukuma et al. (2004) developed a wideband cantilever deflection sensor to measure deflection of vibrating cantilever at high frequency (about 7 MHz). Pinnaduwage et al. (2004) gave a detection method of deflagration of TNT deposited on a piezoresistive microcantilever and pointed out its possible use for explosive-vapor detection. Requa and Turner (2006) reported on the design and experimental measurements of an integrated driving and sensing technique in parametrically excited silicon microcantilevers. Using phase sensitive detection in response to a mechanically chopped excitation source, Wilkinson and Gimzewski (2006) measured the motion of silicon microcantilever. Ghatkesar et al. (2008) measured the resonance frequencies of the eight individual microcantilevers placed in a tiny chamber volume by laser beam deflection detection technique, etc. Also, many publications devoted to the theoretical investigation of the behavior of microcantilevers and several different models were used to describe the vibrations of cantilevers. A linear relation between the displacement of microcantilever was used by Mertz et al. (1993) to control the force incident on a mechanical microcantilever as a function of the monitored cantilever motion by a feedback mechanism. Wilkinson and Gimzewski (2006) showed the fraction of absorbed light within the cantilever varies periodically by using thin film interference modeling and obtained excellent agreement between measurements and simulations. Using Elmer–Dreier model and Sader's extended viscous model, Ghatkesar et al. (2008) estimated the eigenfrequency of nanomechanical cantilevers vibrating in liquid. Using the concept of eigenstrain, Korsunsky et al. (2007) gave models of cantilever deformation to describe inelastic deformation of bimaterial gold-coated microcantilevers, etc. For the vibration of semiconducting cantilevers, which generated by a modulated laser (photothermal excitation), usually the partially coupled system of plasma, thermal and elastic equations was used. For millimeter cantilevers the elastic vibrations spectra calculated agree relatively well with that of experiments (Todorović et al., 1999; Todorović, 2003; Song et al., 2008a,b).

Photothermal (PT) and Photoacoustic (PA) technologies were used widely in investigating the vibration of semiconductors and

* Corresponding author at: MOE Key Laboratory for Strength and Vibration, School of Aerospace, Xi'an Jiaotong University, 710049 Xi'an, People's Republic of China. Tel.: +86 029 82 66 57 06.
E-mail address: yqsong@mail.xjtu.edu.cn (Y. Song).

0020-7683/$ - see front matter © 2010 Elsevier Ltd. All rights reserved.
doi:10.1016/j.ijsolstr.2010.03.020

microelectronic structures due to the merits of non-contact and non-destructive. PA method, while a high sensitivity method, is limited in bandwidth to below 10 kHz and suffers from nonlinear response primarily due to acoustic resonance (Todorović and Nikolić, 2000). The PT method has proved to be a wideband method. In PA and PT experiments the plasma waves, generated by the absorbed intensity-modulated laser beam, can play the dominant role. The thermoelastic (TE) deformation and electronic deformation (ED) are prominent deformations of semiconductors and the main driven mechanisms for micromechanical structures. The thermal waves in the sample cause elastic vibrations. This is the thermoelastic mechanism of elastic deformation. The TE effect is based on the heat generation in the sample and the elastic wave generation through thermal expansion and bending. Conventional theory of thermoelasticity is based on the classical Fourier heat conduction equation. This theory assumes that thermal signal propagates at infinite speeds due to the resulting governing equation is parabolic in nature. This prediction may be suitable for most engineering applications. But for short-pulse laser heating process or under low temperature operating conditions, the conventional thermoelastic model is physically unacceptable because during short work time the thermal cannot obtain equilibrium. So generalized hyperbolic thermoelastic models, which admit a finite speed for propagation of thermal signal, are more suitable to simulate these problems. Among the generalized models, LS model (Lord and Shulman, 1967), with one relaxation time and GL model (Green and Lindsay, 1972), with two relaxation times are familiar to many researchers and many works has been done under these theories (Chandrasekharaiah, 1986; Sharma et al., 2003). The ED mechanism of elastic bending generation is the specific of electronic materials and semiconductors.

The typical dimensions of a microcantilever will be 100 μm long, 10 μm wide, and less than 2 μm thick. Hence it would have a resonance frequency of about 100 kHz. In order to study the microcantilevers vibration characterization near resonance frequencies under optical excitation, partially coupled plasma wave model, thermal wave model with one relaxation time and elastic wave model are used in this paper. The expressions for carrier density, temperature and deflection of silicon microcantilever are obtained analytically. For the temperature and the deflection, the comparisons are made graphically between the results gained from the conventional thermoelastic model and from the generalized thermoelastic model.

2. Formulations of the problem

Consider a semiconducting microcantilever subjected to a homogeneous periodic modulation laser excitation on the surface of cantilever beam. Suppose the cantilever dimension is L in length (x-direction), b in width (y-direction) and h in thickness (z-direction). A general theoretical analysis of the TE and ED effects in microcantilever during photothermal process consists in modeling the complex systems by simultaneous analysis of the coupled plasma, thermal, and elastic wave equations. For a homogeneous semiconducting material, the equations used to describe the photothermal process are now presented.

2.1. Plasma wave

The laser beam excitation generates a depth-dependent plasma wave, which propagates along the thickness of semiconductor cantilever. It is assumed that the density of excess carrier is $n(z,t)$. The excitation energy, E, is greater than the energy gap, E_G, and the absorbed photons generate intrinsic electrons. The excess energy, $\Delta E = (E - E_G)$, is converted by fast non-radiative processes into heat. This electronic diffusion process is characterized by the diffusion coefficient D_E. Also, the excess carriers recombine in the bulk of the crystal, with a characteristic time τ. The so-called Auger recombination time τ is the lifetime of photogenerated electron–hole pairs. The plasma wave equation can be written as (Todorović, 2003)

$$\frac{\partial n(z,t)}{\partial t} = D_E \frac{\partial^2 n(z,t)}{\partial z^2} - \frac{n(z,t) - n_0}{\tau} + I_0(t)(1 - R_s)\frac{\alpha}{2E} e^{-\alpha z}, \tag{1}$$

where n_0 is the equlibrium carrier concentration. The second and third term on the right side in Eq. (1) characterizes the non-radiative Auger recombination and the carrier photogeneration source term, respectively. I_0 is the intensity of the incident optical excitation, which changes periodically with the modulation frequency and R_s is the reflectivity of the sample surface, α is the optical absorption coefficient.

During this diffusion process the carriers can reach the sample surface, with a finite probability of recombination (the surface recombination velocities are s_f, s_r, here f and r represent the front and rear surface of cantilever, respectively). So the boundary conditions, for evaluating the carrier distribution, can be given below:

$$\begin{aligned} &D_E \frac{\mathrm{d}}{\mathrm{d}z} n(z,t)|_{z=0} = s_f n(0,t), \\ &D_E \frac{\mathrm{d}}{\mathrm{d}z} n(z,t)|_{z=h} = -s_r n(h,t), \end{aligned} \tag{2}$$

2.2. Thermal wave

In the case of a solid semiconducting sample excited by a periodic heat source, the resulting temperature oscillations inside the sample have the same mathematical expression as the damped waves, the so-called thermal waves (Salazar, 2006). The thermal waves in the sample cause the elastic vibration. For an isotropic material with constant thermo-physical properties, the thermal transform equation under the generalized thermoelastic LS model can be given as the following form:

$$\begin{aligned} \rho c\left(1 + \tau_0 \frac{\partial}{\partial t}\right)\frac{\partial T(z,t)}{\partial t} = K\nabla^2 T(z,t) + \frac{E_G}{\tau}\left(1 + \tau_0 \frac{\partial}{\partial t}\right)[n(z,t) \\ - n_o] + \varepsilon_T\left(1 + \tau_0 \frac{\partial}{\partial t}\right)\nabla^2 \frac{\partial \mathbf{u}(z,t)}{\partial t} \\ + \left(1 + \tau_0 \frac{\partial}{\partial t}\right)G(z,t), \end{aligned} \tag{3}$$

where ρ, K and c are density, thermal conductivity and specific heat of silicon, respectively; $D_T = K/\rho c$ is the thermal diffusivity; τ_0 is a non-negative constants and referred to as the thermal relaxation time. It represents the time lag needed to establish the steady state of heat conduction in an element of volume when a temperature gradient is suddenly imposed on the element. ε_T is a coupling factor and describes the coupling between thermal wave and elastic waves. In most practical cases this coupling can be neglected. So the temperature distribution is assumed to be completely decoupled from elastic deformation effects. The second term on the right side in Eq. (2) characterizes the effect of heat generation by the carriers recombination in the volume of the sample. $G(z,t)$ is the thermal source term. It was considered as the sum of a thermalization source $G^T(z,t)$, due to photogenerated carriers gives off the excess energy to the semiconductor crystal lattice. This process takes place in a very short time, so this thermal source is also called the fast thermal source; a bulk recombination source $G^{BR}(z,t)$, due to the bulk recombination of the sample as the contribution of the photogenerated carriers transfers heat to the crystal lattice. This thermal source is also called the slow thermal source; and a surface recombination source $G^{SR}(t) = \sum_{i=f,r} G_i^{SR}(t)$ (which is not a function of z), due to the carriers recombination at the front and rear surfaces of the semiconductor layer. These sources can be given in the form below:

$$G^T(z,t) = \gamma_G \frac{\alpha I_o(t)(1-R_s)}{2K} \frac{\Delta E}{E} e^{-\alpha z}, \tag{4}$$

$$G^{BR}(z,t) = \gamma_R \frac{E_G}{K\tau} n(z,t), \tag{5}$$

$$\begin{cases} G_f^{SR} = s_f E_G n(0,t), \\ G_r^{SR} = s_r E_G n(h,t), \end{cases} \tag{6}$$

where γ_G is the carrier generation quantum efficiency, γ_R is the coefficient of bulk recombination ($\gamma_G = \gamma_R \approx 1$).

Boundary conditions for temperature and thermal flux are given by the continuous conditions below:

$$\begin{aligned} &T(0,t) = T_f(0,t), \\ &T(h,t) = T_r(h,t), \\ &K_f \frac{\partial}{\partial z}\left(1+\tau_0 \frac{\partial}{\partial z}\right) T_f(z,t)|_{z=0} = K \frac{\partial}{\partial z}\left(1+\tau_{0g}\frac{\partial}{\partial z}\right) T(z,t)|_{z=0} \\ &\qquad + \left(1+\tau_{0g}\frac{\partial}{\partial z}\right)\left(1+\tau_0\frac{\partial}{\partial z}\right) G_g^{SR}, \\ &K_r \frac{\partial}{\partial z}\left(1+\tau_0 \frac{\partial}{\partial z}\right) T_r(z,t)|_{z=h} = K \frac{\partial}{\partial z}\left(1+\tau_{0g}\frac{\partial}{\partial z}\right) T(z,t)|_{z=h} \\ &\qquad - \left(1+\tau_{0g}\frac{\partial}{\partial z}\right)\left(1+\tau_0\frac{\partial}{\partial z}\right) G_g^{SR}, \end{aligned} \tag{7}$$

here K_i ($i = f,r$) is the thermal conductivity of the medium in front of and in the rear of cantilever surface, respectively. For the case we studied here, $K_f = K_r = K_{air}$. K_{air} is the thermal conductivity of the air, τ_{0g} is the thermal relaxation time for air and $\tau_{0g} \approx 0$.

2.3. Elastic wave

Absorption of the optical energy in a semiconductor microcantilever cause the thermoelastic and electronic deformation. The TE and ED effects are driven mechanisms for microstructure bending. The photogenerated heat can produce elastic deformation in the sample, i.e. TE strain, $\varepsilon^{TE}(z,t)$, it changes proportionally with the change of temperature distribution $T(z,t)$:

$$\varepsilon^{TE}(z,t) = \alpha_T T(z,t), \tag{8}$$

where α_T is the coefficient of linear thermal expansion. Also, the photogenerated plasma can produce a local strain, i.e. electronic strain, $\varepsilon^{ED}(z,t)$, it changes linearly with the change of excess carrier density $n(z,t)$ and can be given by the expression below:

$$\varepsilon^{ED}(z,t) = d_n n(z,t), \tag{9}$$

where d_n is the coefficient of electronic elastic deformation. Since d_n is negative for silicon, it means that electronic strain and thermal expansion strain are opposite in sign. The generation of excess carriers causes a contraction of the material, while thermal heating results in an expansion.

For a thin rectangular microcantilever, the thickness is much smaller than the length and width. The following equation connects the component of elastic strain $\varepsilon_{xx}(x,z,t)$ and the deflection of cantilever $w(x,t)$:

$$\varepsilon_{xx}(x,z,t) = -\frac{\partial^2 w(x,t)}{\partial x^2} z, \tag{10}$$

Component of elastic strain $\sigma_{xx}(x,z,t)$ as a function of the displacement $w(x,t)$, can be obtain from strain–stress relation as following form:

$$\sigma_{xx}(x,z,t) = -E_y\left[\frac{\partial^2 w(x,t)}{\partial x^2} z + \varepsilon^{TE}(x,z,t) + \varepsilon^{ED}(x,z,t)\right], \tag{11}$$

where E_y is Young's modulus.

Dynamic equilibrium of moments gives the elastic moving equation of cantilever as below:

$$\frac{\partial^2 M(x,t)}{\partial x^2} = \rho A \frac{\partial^2 w(x,t)}{\partial t^2}, \tag{12}$$

the moment $M(x,t)$ was given as

$$\begin{aligned} M(x,t) &= b\int_0^h z\sigma_{xx}(x,z,t)dz \\ &= -\underline{B}\left(\frac{\partial^2 w(x,t)}{\partial x^2} + \underline{m}_T(x,t) + \underline{m}_n(x,t)\right), \end{aligned} \tag{13}$$

here $\underline{m}_T = bF\alpha_T m_T/\underline{B},\ m_T = \int_0^h zT(z,t)dz,\ \underline{m}_n = bFd_n m_n/\underline{B},\ m_n = \int_0^h zn(z,t)dz,\ \underline{B} = FI,\ F = E_Y/(1-\nu^2)$,

$I = bh^3/12$,

where $A = bh$ is the section area of microcantilever.

The appropriate boundary conditions, at the clamped side of the microcantilever ($x = 0$) are

$$w(x,t)|_{x=0} = 0, \quad \left.\frac{\partial w(x,t)}{\partial x}\right|_{x=0} = 0 \tag{14}$$

and at the free end of the cantilever beam ($x = L$) are

$$M(x,t)|_{x=L} = 0, \quad \left.\frac{\partial^3 w(x,t)}{\partial x^3}\right|_{x=L} = 0. \tag{15}$$

3. Solution of the problem

3.1. Solution of carrier density

For a modulation laser excitation, the dynamic component of variables (carrier density, temperature and deflection) can be expressed as: $X(\mathbf{r},t) = \underline{X}(\mathbf{r},\omega)e^{j\omega t}$, here $\underline{X}(\mathbf{r},\omega)$ is complex value which defines the amplitude and phase of variables (carrier density, temperature, deflection, etc.) and ω is the angle modulation frequency. According to the governing equation (1) and boundary condition (2), the solution for carrier density can be obtain as following in frequency domain:

$$\underline{n}(z,\omega) = A_+ e^{z/L_w} + A_- e^{-z/L_w} + A_\alpha e^{-\alpha z}. \tag{16}$$

The analytical solutions for the constants A_+, A and A_α are given below:

$$\begin{aligned} &A_\pm = \mp\frac{A_\alpha}{A_L}\left[(1\mp\sigma_f)(1+\delta\sigma_r)e^{-\alpha h} - (1\pm\sigma_r)(1-\delta\sigma_f)e^{\mp h/L_w}\right], \\ &A_L = (1+\sigma_f)(1+\sigma_r)e^{h/L_w} - (1-\sigma_f)(1-\sigma_r)e^{-h/L_w}, \\ &A_\alpha = \frac{I_o(1-R_s)}{2E}\frac{1}{\nu_D}\frac{\delta}{1-\delta^2}, \end{aligned} \tag{17}$$

here $L_w^2 = L_D^2/(1+j\omega\tau),\ L_D = (D_E\tau)^{1/2},\ \delta = \alpha L_w,\ \nu_D = D_E/L_w$ and $\sigma_i = D_E/(s_i L_w)$ ($i = f,r$) is the diffusion length of the excess carriers.

3.2. Solution of temperature

The solution of temperature in frequency domain can be obtained using Eqs. (3)–(7). The periodic components of the temperature distribution in frequency domain induced by three thermal sources can be expressed as

$$\underline{T}(z,\omega) = \underline{T}^T(z,\omega) + \underline{T}^{BR}(z,\omega) + \underline{T}^{SR}(z,\omega) \tag{18}$$

and

$$\underline{T}^i(z) = F_+^i e^{qz} + F_-^i e^{-qz} + F_\alpha^i e^{-\alpha z} \quad (i = T, BR, SR) \tag{19}$$

in which $q(\omega) = (1+j)(1+j\omega\tau_0)^{1/2}/\xi(\omega)$ is the wavenumber of the thermal wave, $\xi(\omega) = (2D_T/\omega)^{1/2}$ is the thermal diffusion. And

$$\begin{aligned}
F_\pm^T &= F_\alpha^T \frac{(r+g)(1\mp g)e^{\mp qh} + (g-r)(1\pm g)e^{-\alpha h}}{(1+g)^2 e^{qh} - (1-g)^2 e^{-qh}},\\
F_\alpha^T &= \frac{I_o(1-R_s)}{2K}\gamma_G \frac{\Delta E}{E}\frac{\alpha(1+j\omega\tau_0)}{q^2-\alpha^2},\\
F_\pm^{BR} &= \frac{(1\pm g)[gC_{BR2} + C_{BR4}] - (1\mp g)[gC_{BR1} - C_{BR3}]e^{\mp qh}}{(1+g)^2 e^{qh} - (1-g)^2 e^{-qh}},\\
F_\alpha^{BR} &= \frac{F_\alpha^{BR} L_w^2}{\alpha^2 L_w^2 - 1},\\
F_\pm^{SR} &= \frac{E_G}{Kq}\frac{s_f n(0)(1\mp g)e^{\mp qh} + s_r n(h)(1\pm g)}{(1+g)^2 e^{qh} - (1-g)^2 e^{-qh}}, \quad F_\alpha^{SR} = 0,\\
C_{BR1} &= L_+ + L_- + L_\alpha, \quad C_{BR3} = \chi[L_+ - L_- - \alpha L_w L_\alpha],\\
C_{BR2} &= -[L_+ e^{z/L_w} + L_- e^{-z/L_w} + L_\alpha e^{-\alpha h}],\\
C_{BR4} &= -\chi[L_+ e^{z/L_w} - L_- e^{-z/L_w} - \alpha L_w L_\alpha e^{-\alpha h}],\\
L_\pm &= \frac{\gamma_R E_G L_w^2}{K\tau q^2(L_w^2 - 1)}A_\pm, \quad L_\alpha = F_\alpha^{BR},
\end{aligned} \tag{20}$$

in which $g = (K_{air}q_{air})(1+j\omega\tau_0)/(Kq)$, $\chi = 1/qL_w$, $r = \alpha/q$.

3.3. Solution of deflection of vibration

The dynamic elastic bending deflection of microcantilever in frequency domain can be obtained using the governing equation (12) and the boundary conditions (14) and (15) as

$$\begin{aligned}
\underline{w}(x,\omega) = \frac{-w_s(L,\omega)}{\eta^2(1+\cos\eta\cosh\eta)}&[-\cos(\eta - k_1x) - \cos(k_1x)\\
&\times \cosh(\eta) + \cosh(\eta - k_1x) + \cos(\eta)\cosh(k_1x)\\
&+ \sin(k_1x)\sinh(\eta) + \sin(\eta)\sinh(k_1x)],
\end{aligned} \tag{21}$$

especially, at the free end ($x = L$) the bending deflection of microcantilever in frequency domain is given as following:

$$\underline{w}(L,\omega) = w_s(L,\omega)F(\omega), \tag{22}$$

in which

$$w_s(L,\omega) = -\frac{L^2}{2}(\underline{m}_T + \underline{m}_n), \quad F(\omega) = \frac{2\sin\eta\sinh\eta}{\eta^2(1+\cos\eta\cosh\eta)}, \tag{23}$$

where $\eta = k_1L$, $k_1 = (\rho A\omega^2/\underline{B})^{1/4}$. The dimensionless dynamic frequency factor $F(\omega)$ approaches 1 when the modulation frequency decreases.

4. Numerical simulation and discussion

We calculate the temperature and the deflection at the front surface in frequency domain, i.e., $\underline{T}(0,\omega)$ and $\underline{w}(0,\omega)$, respectively. The typically parameters of the silicon microcantilever used in these simulations are

$$\begin{aligned}
&\alpha_T = 3\times10^{-6}\ \mathrm{K}^{-1},\ d_n = -9\times10^{-31}\ \mathrm{m}^3,\ R_s = 0.3,\\
&E = 2.33e\ \mathrm{V},\ E_G = 1.11\ \mathrm{eV},\ D_E = 2.5\times10^{-3}\ \mathrm{m}^2/\mathrm{s},\\
&\alpha = 5\times10^5\ \mathrm{m}^{-1},\ \tau = 5\times10^{-5}\ \mathrm{s},\ K = 150\ \mathrm{W/(m\ K)},\\
&D_T = 0.926\times10^{-4}\ \mathrm{m}^2/\mathrm{s},\ \rho = 2.33\times10^3\ \mathrm{kg/m}^3,\\
&c = 695\ \mathrm{J/(kg\ K)},\ E_Y = 1.31\times10^{11}\ \mathrm{N/m}^2,
\end{aligned}$$

For air, the parameters are given below:

$$K_{air} = 0.025\ \mathrm{W/(m\ K)},\ \rho_{air} = 1.205\ \mathrm{kg/m}^3,\ c_{air} = 1013\ \mathrm{J/(kg\ K)}.$$

The length, width and thickness of microcantilever are $L = 100\ \mu$m, $b = 10\ \mu$m and $h = 1\ \mu$m, respectively. The thermal relaxation time is chosen as 0 (corresponding to the case in the classical thermoelastic theory), 10^{-6} s and 5×10^{-5} s (corresponding to the case in the generalized thermoelastic theory).

Fig. 1(a) and (b) shows the change of the amplitude and phase of temperature versus the modulation frequency for different relaxation time. The significant difference can be observed between the results for the generalized and conventional thermoelastic theory. This means that the thermal relaxation time is a very important parameter for the microcantilever's vibrations in the high frequency range. The amplitude of temperature estimated using generalized thermoelastic theory is higher than that using conventional theory. The phase of temperature calculated by using the generalized theory has a phase lag compare with the phase lag obtained with the conventional theory. This phase lag increases when the relaxation time increases. So it can be conclude that the generalized thermoelastic theory (LS model) is more suitable at high modulation frequency.

Fig. 2 shows the amplitude and phase of vibrations calculated by using the generalized thermoelastic theory and conventional theory. Obvious peak can be seen in Fig. 2a. It corresponds to the

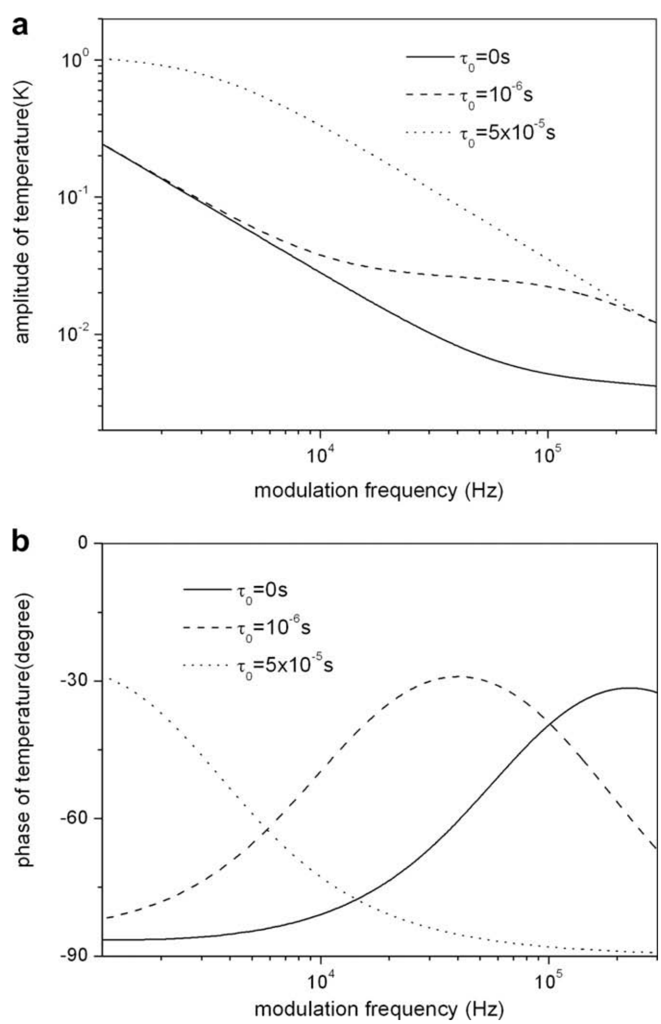

Fig. 1. Amplitude (a) and phase (b) of surface periodic temperature vs. the frequency of modulation: (dashed line and dotted line) the generalized thermoelastic theory; (solid line) the conventional theory.

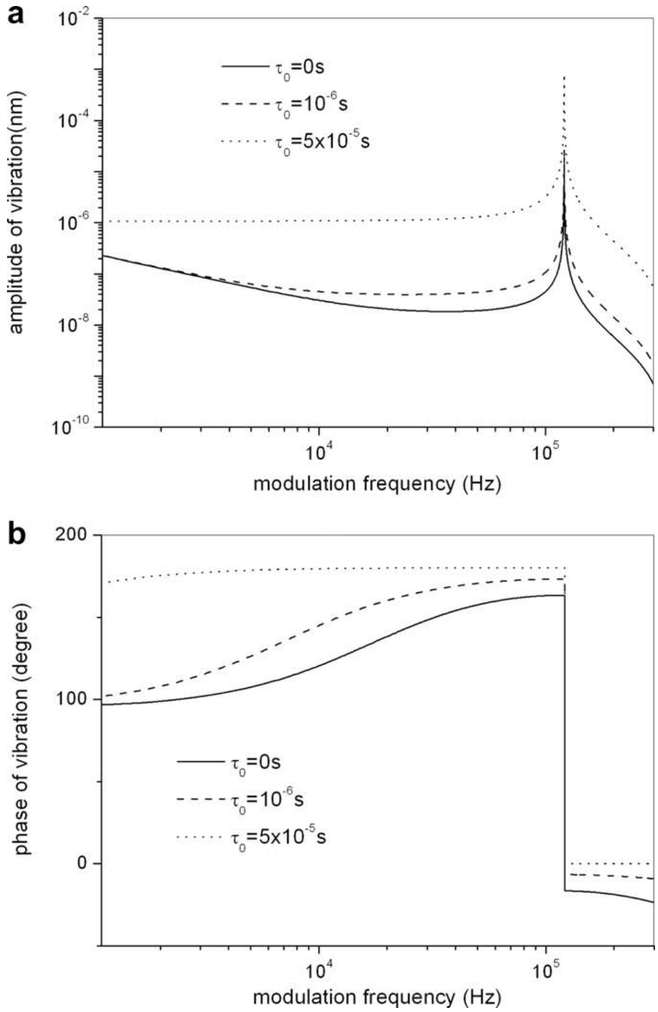

Fig. 2. Amplitude (a) and phase (b) of vibrations vs. the modulation frequency: (dashed line and dotted line) the generalized thermoelastic theory; (solid line) the conventional theory.

resonance frequency of microcantilever. Also the phase curves (Fig. 2b) showed a steep drop by 180° near the resonance frequency. Also it can be see that the amplitude and phase of vibrations calculated by using the generalized thermoelastic theory are higher than those obtained by the conventional theory.

5. Conclusion

The wave-type generalized LS thermoelastic model, along with plasma wave model are used to describe the vibration of silicon semiconducting microcantilevers under periodic laser excitation. The expression of the solution for excess carrier density, temperature and deflection of vibration are obtained analytically in frequency domain. Also the amplitude and phase of temperature and elastic displacement versus modulation frequency for microcantilever are calculated and analyzed. The results of theoretical analysis offer quantitative evidence for the influence of the thermal relaxation time τ_0 to the thermal and elastic waves.

Acknowledgements

The work of Yaqin Song was supported by FFCSA, the National Natural Science Foundation of China (Grant No. 10972169), the Open Foundation of State Key Laboratory of Structural Analysis of Industrial Equipment (GZ0814), SRF for ROCS, SEM and the Foundation of Xi'an Jiaotong University. The work of D.M. Dragan was supported by the Ministry of Science and Technology Development, Republic of Serbia (the project TR 11027). Also the authors would like to thank the referees and the editor for their valuable comments and suggestions.

References

Chandrasekharaiah, D.S., 1986. Thermoelasticity with second sound: a review. Applied Mechanics Review 39, 355–376.

Fukuma, K., Kimura, K., Kobayashi, K., Matsushige, K., Yamada, H., 2004. Dynamic force microscopy at high cantilever resonance frequencies using heterodyne optical beam deflection method. Applied Physics Letters 85 (25), 6287–6289.

Ghatkesar, M.K., Braun, T., Barwich, V., Ramseyer, J.P., Gerber, C., Hegner, M., Lang, H.P., 2008. Resonating modes of vibrating microcantilevers in liquid. Applied Physics Letters 92, 043106.

Green, A.E., Lindsay, K.A., 1972. Thermoelasticity. Journal of Elasticity 2, 1–7.

Korsunsky, A.M., Cherian, S., Raiteri, R., Berger, R., 2007. On the micromechanics of micro-cantilever sensor: property analysis and eigenstrain modeling. Sensors and Actuators A: Physical 139, 70–77.

Lord, H.W., Shulman, Y., 1967. A generalized dynamical theory of thermoelasticity. Journal of Mechanics and Physics of Solids 15, 299–309.

Mertz, J., Marti, O., Mlynek, J., 1993. Regulation of a microcantilever response by force feedback. Applied Physics Letters 62 (19), 2344–2346.

Pinnaduwage, L.A., Wig, A., Hedden, D.L., Gehl, A., Yi, D., Thundat, T., Lareau, R.T., 2004. Detection of trinitrotoluene via deflagration on a microcantilever. Journal of Applied Physics 95 (10), 5871–5875.

Requa, M.V., Turner, K.L., 2006. Electromechanically driven and sensed parametric resonance in silicon microcantilevers. Applied Physics Letters 88. 263508-1-3.

Salazar, A., 2006. Energy propagation of thermal wave. European Journal of Physics 27, 1349–1355.

Sharma, J.N., Kumar, V., Chand, Dayal, 2003. Reflection of generalized thermoelastic waves from the boundary of a half-space. Journal of Thermal Stresses 26, 925–942.

Song, Y.Q., Cretin, B., Todorović, D.M., Vairac, P., 2008a. Study of laser excited vibration of silicon cantilever. Journal of Applied Physics 104. 104909-1-6.

Song, Y.Q., Cretin, B., Todorović, D.M., Vairac, P., 2008b. Study of photothermal vibrations of semiconductor cantilevers near the resonant frequency. Journal of Physics D: Applied Physics 41, 155106.

Todorović, D.M., Nikolić, P.M., Bojičić, A.I., 1999. Photoacoustic frequency transmission technique: electronic deformation mechanism in semiconductor. Journal of Applied Physics 85, 7716–7726.

Todorović, D.M., Nikolić, P.M., 2000, Carrier transport contribution to thermoelastic and electronic deformation in semiconductor. In: Mandelis, A., Hess, P. (Eds.), Semiconductors and Electronic Materials. SPIE Optical Engineering Press, Belingham, Washington, pp. 273–318.

Todorović, D.M., 2003. Plasma, thermal and elastic waves in semiconductors. Review of Scientific Instruments 74 (1), 582–585.

Wilkinson, P.R., Gimzewski, J.K., 2006. Thin film interface in the optomechanical response of micromechanical silicon cantilevers. Applied Physics Letters 89, 241916.